Electrochemical and chemical quantum studies of a natural alkaloid compound: Boldine, as green corrosion behaviour on carbon steel and Copper in sulfuric acid

M. Y. Díaz-Cardenas[1], M. G. Valladares-Cisneros[2*], C. Menchaca-Campos[1], S. Lagunas-Rivera[3], J. G. Gonzalez-Rodríguez[1], J. Uruchurtu-Chavarín[1]

[1]*Centro de Investigación en Ingeniería y Ciencias Aplicadas, Universidad Autónoma del Estado de Morelos, Av. Universidad 1001, Chamilpa, C.P. 62209, Cuernavaca, Morelos, México.*
[2]*Facultad de Ciencias Químicas e Ingeniería Universidad Autónoma del Estado de Morelos, Av. Universidad 1001, Chamilpa, C.P. 62209, Cuernavaca, Morelos, México.*
[3]*Catedra CONACyT, Universidad de Guanajuato, División de Ciencias Naturales y Exactas. C.P. 36050, Guanajuato, Guanajuato, México*

Abstract

The green corrosion behaviour (GCB) of carbon steel and Copper (Cu) were performed in 0.5 M of sulfuric acid, using Boldine such as green corrosion (GC) inhibitor. The electrochemical analysis using different concentrations of Boldine was carried out though Potentiodynamic Polarization Curves (PPC) and Electrochemical Impedance Spectroscopy (EIS). Also, adsorption isotherms, corrosion rates and quantum chemical studies were estimated. The results showed that the GCB of Boldine was better for Cu than carbon steel. The GC inhibition efficiency (GCIE) for Cu through PPC was 87 % observing that Boldine acts as cathodic inhibitor. The GCIE for Cu by EIS was 89 %. The diffusion of ions in the cathodic reaction of Cu diminished by a mixture of physisorption and chemisorption process of Boldine over the metal surface obeying the Langmuir isotherm model, according to the Gibbs free energy. The quantum chemical calculations showed that Boldine favorably adsorbed on Cu surface through the electronegative density atoms such as active centers of adsorption. The theoretical conclusions are agreement with the experimental data reported.
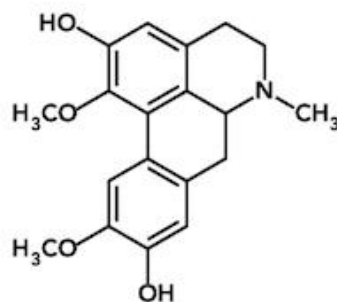
1. Introduction

Corrosion of carbon steel and Copper during acid cleaning plays an important role in mainly industrial process. Sulfuric acid (H_2SO_4), hydrochloric acid (HCl) and nitric acid (HNO_3) are the most commercially available acids, and all of these corrosive media cause metal dissolution during cleaning process [1]. Therefore, corrosion inhibitors have been a good alternative to decrease or prevent corrosion rate in metallic substrates. These substances are added in small concentrations to corrosive media to reduce metal losses. Synthetic commercial organic inhibitors containing heteroatoms in there structures were better option for the industries and, they were widely used in acid environments in the middle of the 20th century [2]. Due to some synthetic and inorganic inhibitor are toxic [3], in recent years the safety regulations are increasing and in the case of aqueous cleaners recommend preferably use of safe clean chemicals and reduce the wastes to produce in cleaning processes [4].

Therefore, greats efforts have been done about searching for new corrosion inhibitors [5, 6]. It has also been studied organic substances from natural sources in different media for various metals [7-11]. In the case of extracts from plants, studies have been demonstrated that they are a good alternatives [6, 12-17]. Recently some alkaloids have been studied as corrosion inhibitors by electrochemical

techniques, adsorption isotherms, quantum chemical studies and weight loss. The study as green corrosion inhibitor of alkaloids extract from *Retama monosperma* stems (AERMS) on carbon steel in 1 M HCl mentioned that AERMS inhibited the corrosion efficiently more than 80 % [18]. Also, the alkaloid fraction of the ethanol extract from *Costus afer* (AECA) was reported with properties as green corrosion inhibitor of mild steel in 5 M HCl by gasometric and gravimetric techniques [19].

The methanol extract of *Peumus boldus (P. boldus)*, which in a previous report it was demonstrated to be a potential corrosion inhibitor [20], due to the presence of aromatic compounds as alkaloids. Alkaloids like Boldine and their derivatives [21] are found in the leaves of *P. boldus* and, they have been shown effective hepato-protective action also due to their antioxidant activity [22, 23]. The chemical structure of Boldine is given in Figure 1.

Figure 1. Chemical structure of the natural alkaloid Boldine (Molecular weight 327.37 g/mol)

Taking as reference the principal components of *P. boldus* extract, the main objective of this work is to evaluate the inhibitory effect of Boldine on the corrosion of carbon steel and Copper, in H_2SO_4 0.5 M using electrochemical techniques, adsorption isotherms and quantum calculations.

2. Material and Methods

2.1. Preparation of metal electrodes

Cylindrical probes with diameter of 0.6 mm of Copper and carbon steel (0.14% C, 0.90% Mn, 0.03% P and balance Fe) with a Copper wire spot welded on them, were encapsulated in a commercial polymeric resin. The exposed area was 0.28 cm^2 which was abraded with 600 SiC emery paper.

2.2. Testing solution

It was used H_2SO_4 at 98% analytic grade, Boldine which was purchased from Aldrich and used without further purification, and distilled water.

The corrosive media was made diluting sulfuric acid in distilled water to obtain a concentration of 0.5 M. Also, Boldine was prepared in a concentrated solution to be added in the corrosive media and obtain five different testing concentrations (0.010, 0.050, 0.100, 0.300 and 0.500 g/L). All electrochemical cells were carried out at 25 ºC in open atmosphere.

2.3. Parameters of electrochemical tests

Potentiodynamic polarization curves (PPC) and Electrochemical Impedance Spectroscopy (EIS) measurements were used. For EIS tests, the amplitude applied for the signal was 20 mV. Also, the frequency interval was of 10 KHz to 0.01 Hz. Each specimen for the PPC were taken in a potential range of ± 500 mV around the open circuit potential, with a scan rate of 1 mV/s. The values of corrosion current density for carbon steel were calculated by Tafel cathodic slope extrapolation. On the other hand, the corrosion current density for Copper was calculated by anodic Tafel slope.

All experiments were carried out using a fully automated protentiostat/galvanostat from ACM instruments. A saturated Ag/AgCl reference electrode and graphite rod as auxiliary electrode were used. In each assay was reached a steady-state value, immersing each specimen into the solution during 20 min. All the experiments were repeated three times.

3. Results and discussion

3.1. Potentiodynamic Polarization Curves (PPC) for carbon steel

The carbon steel behaviour on PPC curves in absence and in the presence of different concentrations of Boldine is observed in Figure 2, were the corrosion potential shifted to more negative values for low concentrations (0.010, 0.050, and 0.100 g/L). This behaviour is may be due to the active state in the presence of the alkaloid, which favours the polarization of the anodic reactions, and promotes the dissolution of carbon steel [24]. The cathodic branch is reduced, and the slopes were modified in the presence of Boldine. It could be due to the alkaloid influences strongly the cathodic reduction reaction, although, Boldine can be classified as cathodic inhibitor [25].
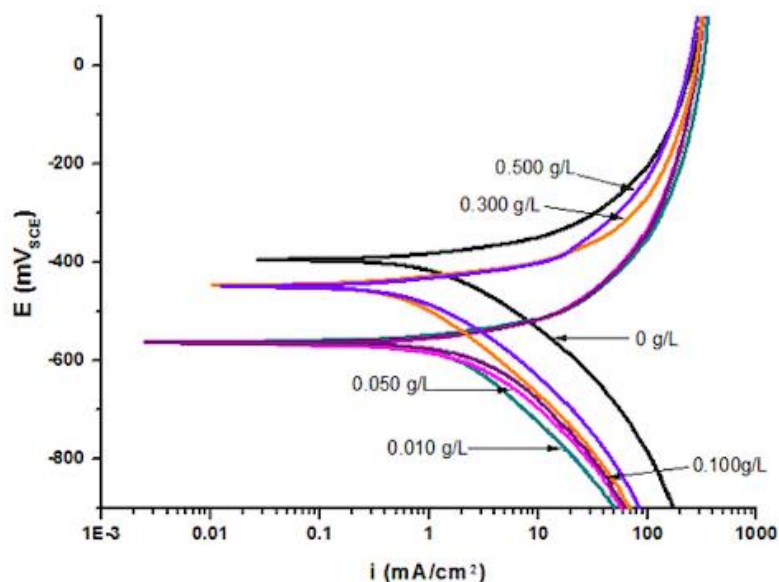

Figure 2. PPC for carbon steel in the presence of different concentrations of Boldine in H_2SO_4 0.5 M at 25 °C in open atmosphere.

However, carbon steel in the presence of the highest concentrations (0.300 and 0.500 g/L) showed that the cathodic E_{corr} value changed near to the blank value decreasing the polarization of the anodic reaction. Therefore, the current density is diminished as can be seen in Table 1.

The corrosion rate *CR* (mm/yr) values from PPC were calculated using equation 1, assuming that the whole metal surface is attacked by uniform corrosion:

$$CR = K \frac{I_{corr}}{d} \text{ EW} \tag{1}$$

where I_{corr} is the corrosion current density ($\mu A/cm^2$), *d* represents the density (7.874 g/cm^3), *K* is a constant (3.27 x 10^{-3} mm g/μA cm yr), EW is the equivalent weight of carbon steel [26].

Also, the corrosion inhibition efficiency percent (CIE %) was calculated with the following equation:

$$CIE \% = \frac{I^0_{corr} - I_{corr}}{I^0_{corr}} \times 100 \tag{2}$$

where I_{corr} represents the corrosion current density in the presence of Boldine and I^0_{corr} is the current density obtained from the blank sample.

Taking into account the dissolution of iron in acid solution at equilibrium, where the total cathodic rate is equal to the total anodic rate [27], the parameters were calculated with cathodic Tafel slope (βc) extrapolation [28] (see the supplementary information), due to the anodic Tafel slope is not visible due to the anodic dissolution does not displays Tafel region zone and the anodic branch presented and active/passive transition [29, 30]. Therefore, anodic curve did not present well-defined Tafel region. According to these parameters, Boldine presented the highest efficiency (71%) for carbon steel at 0.300 g/L.

Table 1. PPC Electrochemical parameters of carbon steel in the presence Boldine in acid solution at 25 ºC in open atmosphere

Boldine		I_{corr}	$-E_{corr}$	$-\beta c$	CR	CIE %
g/L	$X10^{-3}$ M	(mA/cm^2)	(mV)	(mV/dec)	(mm/yr)	
0	**0**	1.9	393	218	3.08 x10^{-5}	-
0.010	**0.0305**	1.3	558	181	2.08 x10^{-5}	31
0.050	**0.1527**	1.4	566	167	2.95 x10^{-5}	26
0.100	**0.3054**	1.6	562	131	3.95 x10^{-5}	16
0.300	**0.9163**	0.5	443	172	6.26 x10^{-6}	71
0.500	**0.5273**	0.7	445	171	9.74 x10^{-6}	63

3.2. EIS measurements for carbon steel

The overall impedance for carbon steel is represented in Nyquist and Bode plots in the presence of different concentration of Boldine (Figure 3). It is possible to observe a depressed capacitive semicircle at the higher frequency range, followed by an inductive loop at low frequencies [31] in the Nyquist plots in all concentrations. This phenomenon is corroborated in the Bode plots (Figure b), where the phase angle presents at least two time constants. These can be due to more than one process occurring on the metal surface. The capacity loop in the high frequency range can be due to the heterogeneity of the surface an adsorption process [32]. Also, the inductive loop can be attributed to the relaxation of adsorbed species as H^+_{ads} [25].
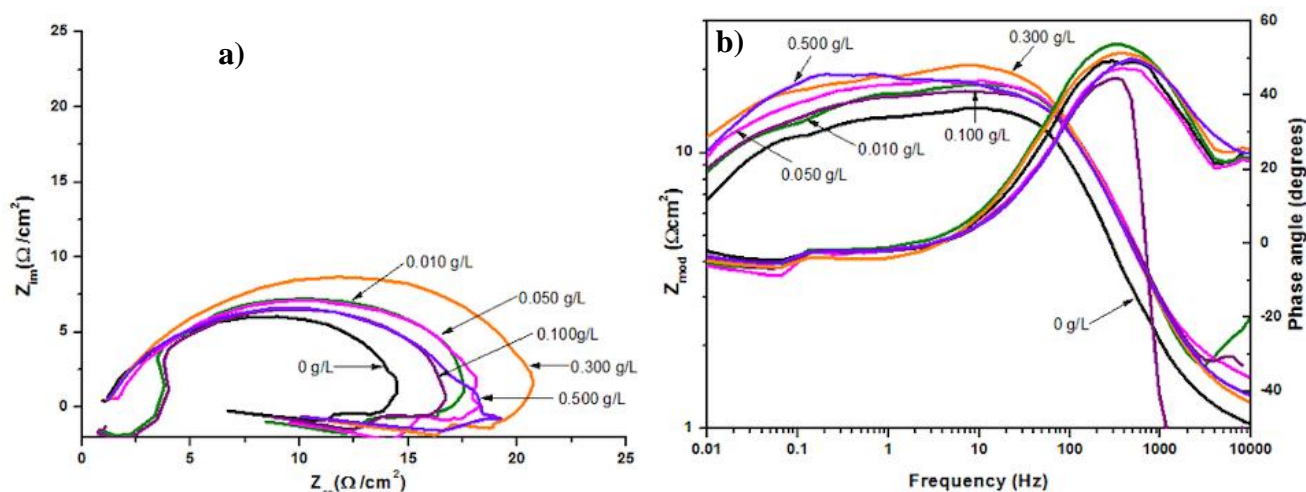

Figure 3. Carbon steel behaviour in H_2SO_4 0.5 M and Boldine at 25 ºC by EIS technique
a) Nyquist and b) Bode plots.

The equivalent circuit presented in Figure 4, can be used to analyse and fit all impedance data obtained, because the addition of Boldine does not alters the mechanisms for the metal dissolution, that is to say, equivalent circuit fits in the same way in the presence of inhibitor and in the blank sample. As an example, it is shown experimental and simulated data for carbon steel in H_2SO_4 0.5 M. According to the equivalent circuit model was obtained electrochemical parameters such as R_s that represents the solution resistance, C_{dl} is the double-layer capacitance, the effect of the organic compound for carbon steel at high frequencies represents the capacitive loop, R_{ct}-C, and RL-L are in parallel and represents the inductive loop at low frequency. According to Poorqasemi *et al.* [33] the capacitive loop is attributed to the charge transfer reaction. Also, the inductive loop (RL-L) observed at low frequencies is attributed to a relaxation process by the adsorption of ions from the electrolyte over the metal surface. Moreover, Lorenz and Mansfeld [34] suggest that the inductive loop which has not a perfect semicircle shape in low frequency is a phenomenon observed for iron in acidic media (0.5 M H_2SO_4) that depends on the nature of the acid, the additive, time and potential. This inductive loop can disappear after log times of

immersion. According to the suggestions made by these authors, in this work the effect of the organic compound was analysed in the first 2 hours of immersion.
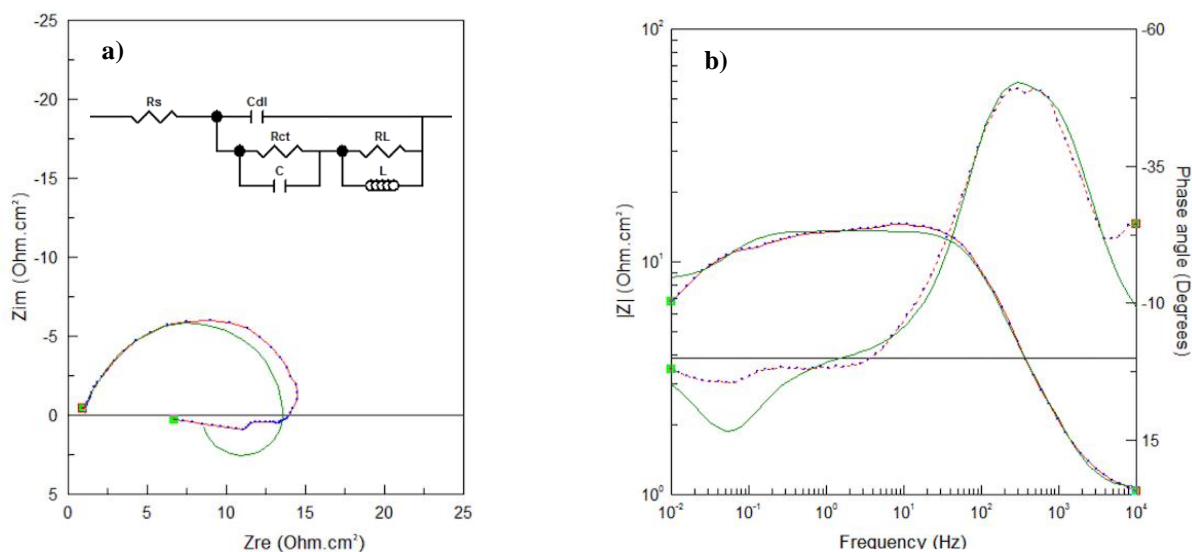

Figure 4. Electric circuit fitted for carbon steel in H$_2$SO$_4$ 0.5 M in absence and in the presence of Boldine in open atmosphere: a) Nyquist and b) Bode plots (····) experimental; (—) calculated.

The parameters calculated for EIS technique according to the circuit fit can be seen in Table 2. When an inductive loop appears at low frequencies, the polarization resistance (R$_p$) can be calculated from equation 3 [35].

$$R_p = \frac{R_L \times R_{ct}}{R_L + R_{ct}} \tag{3}$$

Therefore, the CIE % value was calculated from R$_p$ data as in the following equation [25].

$$CIE \% = \left(1 - \frac{R_p^0}{R_p}\right) \times 100 \tag{4}$$

where R^0_p and R$_p$ are the polarization resistance in absence and in the presence of Boldine respectively. Also, in Table 2 is observed that generally C$_{dl}$ decreased according to the increase of the R$_p$ value, and the more inductance L increases, the more CIE increase, obtaining the best efficiency (65%) at 0.300 g/L.

Table 2. EIS parameters of carbon steel in presence of Boldine in acid solution at 25 ºC in open atmosphere.

Boldine		R$_s$	C$_{dl}$	R$_{ct}$	C	RL	L	R$_p$	CIE
g/L	X10^{-3} M	(Ω/cm²)	(µFcm^{-2})	(Ω/cm²)	(µFcm^{-2})	(Ω/cm²)	(Henri/cm²)	(Ω/cm²)	%
0	**0**	1.07	92.64	7.89	128	5.19	11.80	3.13	-
0.010	**0.0305**	3.09	110.00	14.69	2,517,000	10.71	82.38	6.19	49
0.050	**0.1527**	1.79	81.84	13.31	1,512,000	14.98	134.80	7.05	56
0.100	**0.3054**	3.28	117.00	11.58	1,857,000	10.23	61.64	5.43	42
0.300	**0.9163**	1.41	82.50	18.67	1,255,000	17.08	164.70	8.92	65
0.500	**0.5273**	1.43	55.52	16.01	1,320,000	15.88	150.90	7.97	61

The effect of L is related to the RL, when the latter increases L also increases. Both inductive elements represent deposition of surfaces layer. It is clear that there are interactions between Boldine

and corrosion products. The surface layer influences parameter C, which increased with the addition of inhibitor that generally shows that the more efficiency the less C value is observed. Therefore, inductive behaviour can occur due to the stabilization of corrosion products by interactions with inhibitor molecules as well as by re-dissolutions of the passive film [36].

3.3. PPC curves for Copper

The anodic and cathodic PPCs of Cu in sulfuric acid were shown in Figure 5. The cathodic polarization curve of Copper into sulfuric acid can be divided into three regions according to the reduction of oxygen process [37]. At high overpotentials (-500 mV to -400 mV), is observed the limit current by the oxygen diffusion reaction. Overpotential between -400 mV and -200 mV, the mixed kinetic-diffusion control occurs, and the hump with the maximum current density appear from -200 mV to -50 mV. Then, the limit current of Copper at high overpotentials and the mixed kinetic diffusion control were also observed in the presence of Boldine, attributed to the diluted oxygen influences on the behaviour of the cathodic branch. However, in the presence of 0.300 g/L and 0.500 g/L, the corrosion potential shifted -100 mV more than the blank sample, consequently, the cathodic hump disappeared.
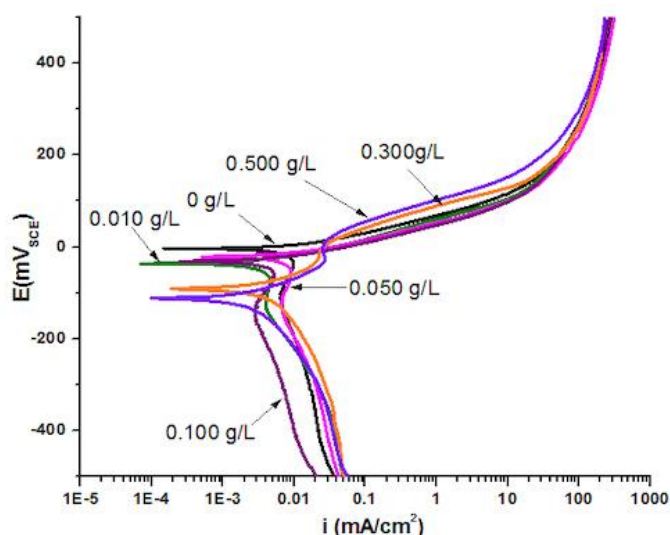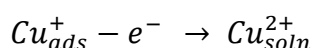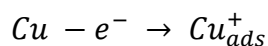

Figure 5. PPC of Copper in the presence of different concentration of Boldine in sulfuric acid at 25ºC in open atmosphere.

On the other hand, the anodic curve in the presence of low concentrations of Boldine (0.010, 0.050, 0.100 g/L) remained unchanged. Nevertheless the presence of 0.300 and 0.500 g/L of the alkaloid reduced the anodic current density, may be due to Boldine like other organic compounds is adsorbed over the metal surface at potentials close to the E_{corr} [38]. It is known that the general mechanism of Copper dissolution in sulfuric acid is given as follows [39]:

$$Cu - e^- \rightarrow Cu_{ads}^+$$

$$Cu_{ads}^+ - e^- \rightarrow Cu_{soln}^{2+}$$

The first step of Copper dissolution is carried out faster than the second step. The last is considered the rate limiting due to cuprous ions remain on the surface and do not diffuse into the solution, so that is not present the cathodic Tafel slope showing a vertical line from limiting current density (I_L). The cathodic process is regularly observed for Copper in 0.5 M of H_2SO_4 [40] and is related to the oxygen dissolved reduction [41]. Table 3 lists the electrochemical parameters from PPC, current density (J_{corr}) and corrosion potential (E_{corr}) were obtained from extrapolation of the anodic Tafel slope. The CIE % and CR values were calculated from J_{corr}. The anodic Tafel slope for Copper into sulfuric acid (37 mV/dec) is consistent with the diffusion of cupric ions is the dominant process [39, 42]. Also, Cu in the

presence of low concentrations of Boldine (0.010, 0.050 and 0.100 g/L) generally remains with constant values considered as diffusion of cupric ions as the dominant process. However, a considerably increment of the anodic Tafel slopes of Boldine at high concentrations (0.300 and 0.500 g/L) is seen, this behaviour suggests the diffusion is not dominant due to the alkaloid affects the cathodic reaction changing the E_{corr} to more negative values [44]. The change in the E_{corr} value allows an inhibitor to be classified as cathodic or anodic type [45]. The change in the E_{corr} (87 mV) by the presence of Boldine it is noted at 0.300 g/L, this concentration produces an E_{corr} of 91 mV, and when the concentrations of Boldine is 0.500 g/L the E_{corr} change increases until 105 mV reaching 87 % of CIE and the CR is reduced as well. Table 3 clearly shows that increasing the concentration of Boldine, the corrosion current density (j_{corr}) decreases, therefore, the higher efficiency was 87% at 0.500 g/L.

Table 3. PPC Electrochemical parameters for Cu in the presence of Boldine in acid solution at 25 °C in open atmosphere.

Boldine		I_{Lim}	$-E_{corr}$	J_{corr}	βa	CIE	CR
g/L	X10^{-3} M	(mA/cm^2)	(mV)	(mA/cm^2)	(mV/dec)	%	(mm/yr)
0	**0**	0.004	4	0.015	37	-	3.50 x 10^{-4}
0.010	**0.0305**	0.005	34	0.008	38	47	1.87 x 10^{-4}
0.050	**0.1527**	0.002	21	0.007	33	53	1.63 x 10^{-4}
0.100	**0.3054**	0.001	30	0.006	31	60	1.40 x 10^{-4}
0.300	**0.9163**	0.005	91	0.003	59	80	7.00 x 10^{-5}
0.500	**0.5273**	0.002	109	0.002	68	87	4.67 x 10^{-5}

3.4. EIS measurements for Copper

It is observed a depressed semicircle in the high frequency region with one capacitive time constant in the Bode-phase diagrams (Figure 6) associated with the double electric layer and charge transfer resistance, attributed to the Copper dissolution [46].
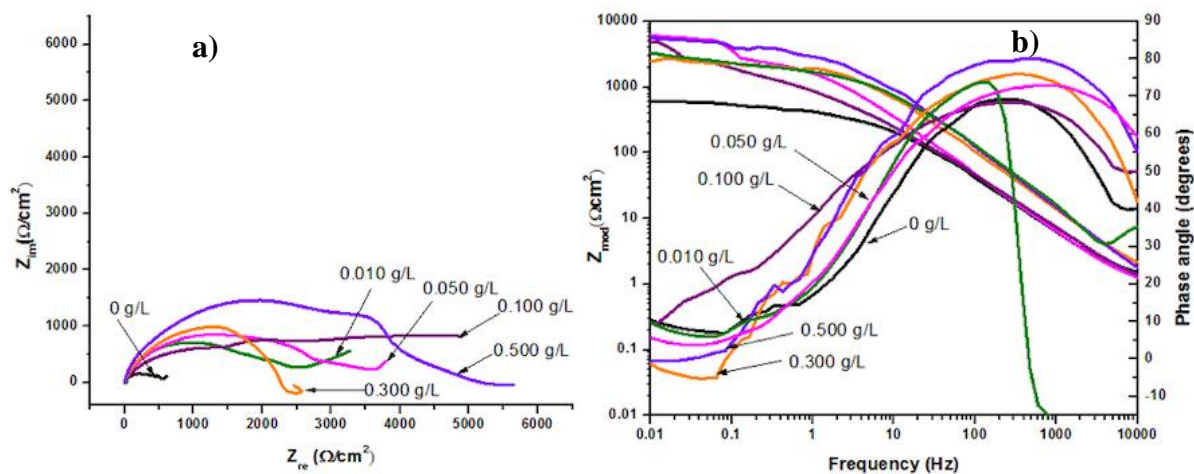

Figure 6. Impedance plots for Cu in the presence of Boldine in H$_2$SO$_4$ 0.5 M. at 25 °C in open atmosphere.
a) Nyquist and b) Bode plot.

At low frequencies, the blank sample showed a Warburg response appeared, that indicates the diffusion controlled process can occur through the dissolved oxygen reduction reaction on Copper surface. The systems of Cu in the presence of different concentrations of Boldine presented the diffusion phenomenon at low frequencies as well. The shape in the impedance plots reminds similar throughout all tested concentrations. However, at 0.300 and 0.500 g/L in the high frequency region is clearly observed that the impedance takes semicircle shape, due to the capacitive behaviour becomes more dominant than diffusional component. It can be attributed to the adsorption of Boldine over Cu surface. Also the more increase the concentration, the more increase diameter of the capacitive semicircle.

The equivalent circuit fit (Figure 7, representative example) shows impedance elements such as R_s represents the charge transfer resistance, CPE is the phase constant element associated with double layer capacitance [47], and W indicates the diffusional impedance.
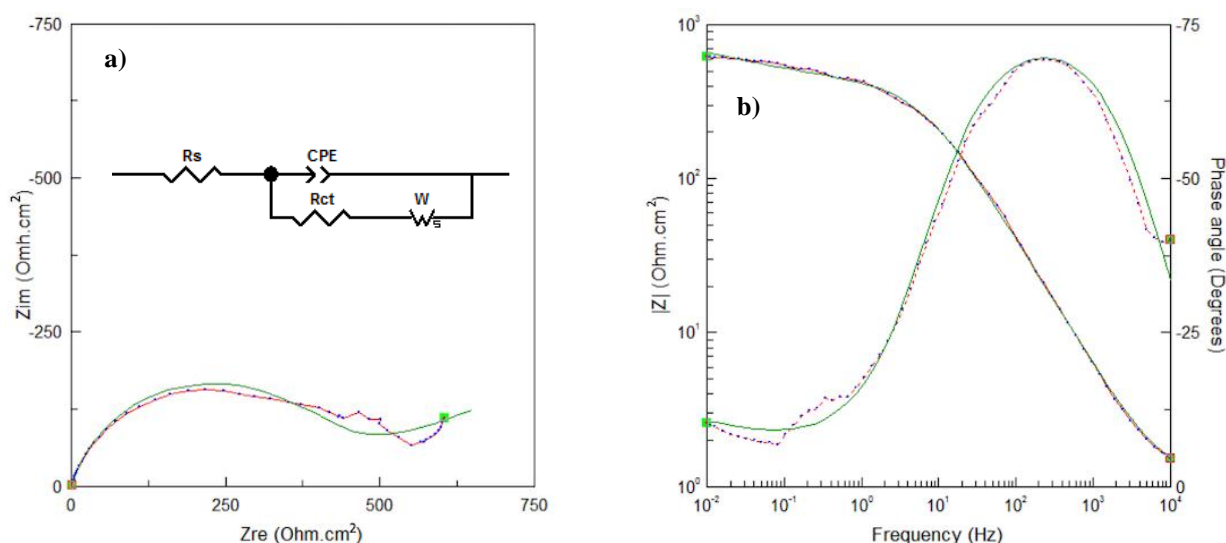

Figure 7. Equivalent circuit fitted for Copper in H_2SO_4 0.5 M in absence and in the presence of Boldine in open atmosphere: a) Nyquist and b) Bode plots ($\cdots$) experimental; ($\longrightarrow$) calculated.

Table 4 lists the electrochemical parameters obtained from the circuit fit data, where is observed a diffusional component (W) increase according to the impedance is influenced by the non-diffusional component [48]. Parameters as R_{ct} increases according to CPE value decreases. It can be observed when the molecules of water are replaced by organic molecules through adsorption over the metal surface, causing diminishing of the local dielectric constant and increasing the double layer thickness. The increment of the double layer is related with the surface roughness and heterogeneity that could be corroborated with the variation observed for the *n* value [49, 50].

Table 4. EIS Electrochemical parameters for Cu in the presence of Boldine in acid solution at 25 °C in open atmosphere.

Boldine		R_s (Ω/cm^2)	CPE ($\mu F cm^2 s$)	*n*	R_{ct} (Ω/cm^2)	W (Ω/cm^2)	CIE %
g/L	X10^{-3} M						
0	**0**	1.2	81.5	0.83	364	824.5	-
0.010	**0.0305**	16.7	30.9	0.91	1529	874.0	76
0.050	**0.1527**	0.8	70.3	0.87	2097	0.40	83
0.100	**0.3054**	0.5	70.3	0.88	1802	6.10	80
0.300	**0.9163**	1.3	35.6	0.88	2287	147.4	84
0.500	**0.5273**	1.0	17.0	0.94	3547	1508	89

3.5. Adsorption isotherms

Taking into account that even the most carefully polished surfaces, are not smooth in microscopic sense, but are irregular with valleys and peaks altering over the surface. The areas of irregularity are usually susceptible to residual fields' forces. At these locations the surface atoms of the metal may attract other atoms or molecules in the surrounding gas or liquid phase, in this case molecules such as oxygen or Boldine. Therefore, two types of adsorption can occur: physical adsorption and chemisorption [51].

In this work the calculations for the adsorption isotherms were carried out using the values from PPC and EIS techniques. After to determine fits using different isotherms we were tried, as they are the most frequently used: Langmuir, Temkin, Frumkin, and Freundlich [52, 53]. The best correlation

coefficients (R^2) were obtained with the Langmuir model where C/θ is plotted in function of the concentration (C) as can be seen in Figure 8 [54, 55].
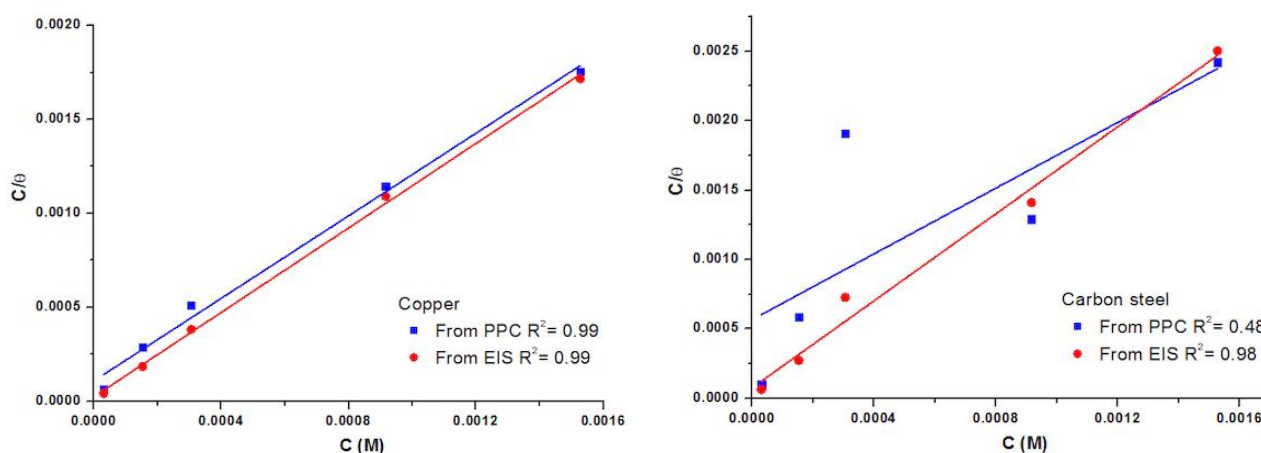

Figure 8. Langmuir adsorption isotherms for Copper and carbon steel calculated from PPC and EIS

The free energies of adsorption -ΔG^0_{ads} were calculated by the following equation:

$$\Delta G^0_{ads} = -RT \ln(55.5)K_{ads} \tag{3}$$

where R is the universal constant of gases and T is the absolute temperature and, value 55.5 M^{-1} is the molar concentration of water in the solution [56].

The energies of adsorption showed in Table 5 suggest that Boldine is adsorbed over the metal surface. The physical adsorption is given when the forces attracting the fluid molecules to the solid surface are relatively weak, due to the fact that the forces involved in this process are weak. According to this fact, usually values of -ΔG^0_{ads} of the order of 20 $KJmol^{-1}$ or lower, are consistent with a physisorption. Also, values of the order of 40 KJ mol^{-1} or higher are associated with chemisorption [57].

Table 5. Values of K_{ads} and -ΔG^0_{ads} for carbon steel and Copper, from fitting EIS and PPC curves data according to Langmuir isotherm adsorption.

Metal	Test data	R^2	K_{ads} M^{-1}	$-\Delta G^0_{ads}$ KJ mol^{-1}
Copper	PPC	0.99	359.72	24.55
	EIS	0.99	381.73	24.59
Carbon steel	PPC	0.48	386.30	24.72
	EIS	0.98	513.97	25.43

The -ΔG^0_{ads} energies showed in Table 5 suggests that Boldine presented a mixed process between physisorption and chemisorption over the metal surface, either carbon steel or Copper, due to physisorption is a stage preceding chemisorption. This behaviour is observed in organic molecules which act forming chelates with the positive ions of metal [58]. The calculation of the adsorption equilibrium constant K_{ads} allowed to get the standard free energy, for Copper and carbon steel in the presence of Boldine were in both techniques, around -24 KJ mol^{-1}; these results confirmed that Boldine interacts on the Copper and carbon steel surface by a mixture process between physisorption and chemisorption [59].

3.6. Quantum chemical calculations

To corroborate the effect of Boldine over the metal surface of carbon steel and Copper, it was considered essential to study the flavonoid by quantum calculations. The optimized molecular structure is presented in Figure 9, with the highest occupied molecular orbital (HOMO), and the lowest occupied

molecular orbital (LUMO) of Boldine, where is clearly observed similar molecular orbital distributions HOMO and LUMO, because they are distributed around the all rings of Boldine. Owing to the frontier orbitals are the principal factor to obtain a reaction, for a molecule E_{HOMO} is frequently associated with the ability to donate electrons.

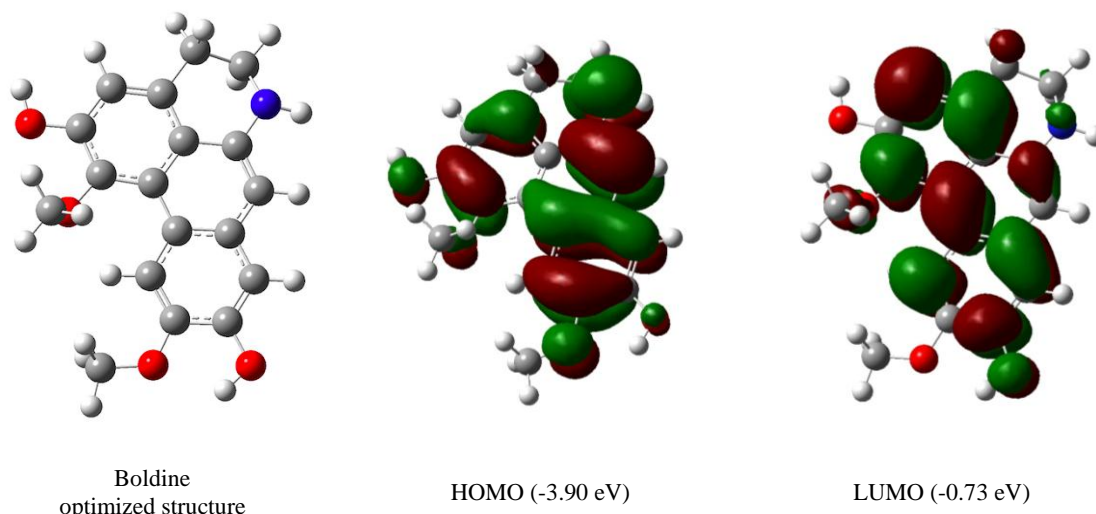| Boldine optimized structure | HOMO (-3.90 eV) | LUMO (-0.73 eV) |

Figure 9. Frontier molecular orbital density distribution for Boldine obtained using DFT at the B3LYP/6-631(*d*).

The adsorption of a molecule over the metal surfaces is carried out between the π-electrons from the heteroatoms of the inhibitor and the vacant *d*-orbitals of the metal surface [60]. Therefore, a molecule with higher E_{HOMO} and the lowest ΔE (E_{HOMO}-E_{LUMO}) is often associated with inhibition efficiency. In this work, Boldine presented the best efficiencies for Cu (89% at 0.500 g/L) agree on the adsorption and chemisorption process observed by isotherms calculations. Also, this alkaloid presented E_{LUMO} (-0.73 eV) associated with the ability to receive electrons. It suggests that Boldine accepts electrons from the metal surface through its antibonding orbitals [61]. These could be to the presence of nitrogen (N) and hydroxyl groups (OH) on the rings.

On the other hand in Table 6, the dipole moment (**μ**) is another important indicator to predict the interaction of the corrosion inhibition, due to the dipole moment gives the direction of the electronic distribution around of the molecule [62] and it is related to the total charge distribution and electronegativity. It is important to highlight that as can be seen in Figure 10, the alkaloid Boldine presents four heteroatoms of oxygen and one more heteroatom of nitrogen distributed around the rings with a dipole moment value **μ** = 4.79 Debye. It suggests that the distribution of the electronegative atoms into the rings corresponds to the active sites which are highly active receptor bindings because the larger the dipole moment the stronger will be the intramolecular attraction [63].
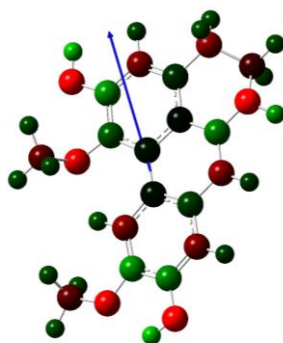

Figure 10. Dipole moment direction for Boldine molecule.

Others helpful properties that they can be obtained by quantum calculations are absolute hardness (η) and softness (σ). These parameters are related with the ΔN, where the relationship denotes that hard

molecules presented large ΔE and, soft molecules have small ΔE [64], and as ΔE decreases the reactivity of molecule increases allowing corrosion inhibition [65]. According to the above, Boldine presented ΔE = - 3.17eV and the largest η = 1.5 eV. These parameters suggest that Boldine is a soft molecule with high reactivity and it could offer electrons to carbon steel an acceptor system, may be by adsorption process.

Table 6. Molecular properties of the alkaloid Boldine obtained from DFT calculations at the B3LYP/6-631(d).

Parameter	Boldine
Total E (eV)	28620.95
E_{HOMO} (eV)	-3.90
E_{LUMO} (eV)	-0.73
ΔE (eV)	-3.17
Dipolar moment **μ** (Debye)	4.79
Hardness **η** (eV)	1.50
Softness **σ** (eV)	0.67
Electronegativity χ (eV)	2.31

The number of transferred electrons ΔN is related with the reactivity for explaining the chemisorption bonding trends, and it can be calculated by the following equation.

$$\Delta N = \frac{\chi_{Me} - \chi_{inh}}{2(\eta_{inh})}$$

Where χ_{Me} is the absolute electronegativity of metal (either Fe or Cu) and χ_{inh} represents the absolute electronegativity of alkaloid Boldine. Also η_{inh} is the absolute hardness of Boldine.

Taking into account the theoretical values for the metals studied in this work, the absolute electronegativity values considered for each metal are for Fe $\chi_{Fe} = 4.28$ eV and for Cu is $\chi_{Cu} = 3.46$ eV as suggested in the literature [66]. The value obtained of transferred electrons for Fe in the presence of Boldine was ΔN = 0.65 eV and Cu in the presence of Boldine presented ΔN = 0.79 eV, as is clearly seen, both ΔN for Fe and Cu were positive values, it is known that ΔN > 0 means that a molecule transfer electrons. However, if ΔN < 0 the molecules cannot transfer electrons [67]. Boldine presents ability to transfer electrons, consequently these results are according to the highest ΔN value which was obtained for Copper in presence of Boldine, also the best inhibitions efficiencies were obtained for Copper. The latter suggests the mechanism of inhibition is partially influenced by chemisorption as can be corroborated with the isotherm model.

It is possible to conclude that the green corrosion inhibition efficiency of Boldine was better on copper surface than carbon steel surface, due to two important issues: 1) the interaction between Copper and Boldine (ΔN = 0.79 eV) was better than carbon steel and Boldine (ΔN = 0.65 eV), these are evidenced by the value of number of transferred electrons (ΔN) thus allowing Boldine to have a higher affinity on the Copper surface; 2) because chemisorption is as slow process as the second step of copper dissolution reaction in acidic medium, so that Boldine can be adsorbed at the active sites of Cu^{1+} and Cu^{2+} ions on the surface.

Conclusion

The results obtained in this study of Boldine as green corrosion inhibitor for carbon steel and Cu in 0.5 M of H_2SO_4 in open atmosphere conditions showed that, Boldine presented more efficiency for Cu compared with carbon steel system.

According to PPC and EIS tests in open atmosphere conditions for Copper, Boldine acted as cathodic inhibitor type, being adsorbed by a mixture of physisorption and chemisorption on metal surface as suggested by the correlation of Langmuir isotherm. 0.500 g/L Boldine gives the bether CIE

for Cu (89 % by EIS and 87 % by PPC) than carbon steel (61 % by EIS and 63 % by PPC). Boldine changed from diffusional dominant process to capacitive allowing an increment for the charge transfer resistance, these were observed and corroborated by EIS technique.

The parameters calculated through DFT showed that the distribution of HOMO and LUMO energies of Boldine were uniform distributed through hydroxyl groups (OH) and nitrogen (N) atom present into the rings corroborating that the inhibition mechanism can occur though physisorption and partially chemisorption.

References

1. G. Schmitt. *Br. Corros. J.*, 19 (1984) 165-176. https://doi.org/10.1179/000705984798273100
2. S. Hooshmand Zaferani, M. Sharifi, D. Zaarei, M. R. Shishesaz. *J. Environ. Chem. Eng.,* 1 (2013) 652-657. https://doi.org/10.1016/j.jece.2013.09.019.
3. N. M. Dummer. *Rev. Environ. Sci. Biotechnol.,* 13 (2014), 53-61. https://doi.org/10.1016/j.jece.2013.09.019.
4. M. C. McLaughlin, M. A. Alan, S. Zisman. Aqueous Cleaning Handbook Aqueous Cleaning Handbook, techniques, AI Technical Communications, USA, ISBN: 0-9723478-1-X(2005), Library of Congress Catalog Card Number 200211064.
5. P. B. Raja, M. G. Sethuraman, *Mater. Lett.*, 62 (2008) 113-116. https://doi.org/10.1016/j.matlet.2007.04.079.
6. G. Chen, M. Zhang, J. Zhao, R. Zhou, Z. Meng, J. Zhang. *Chem. Cent. J.*, 7 (2013) 1-7. https://doi.org/10.1186/1752-153X-7-83
7. M. Znini, L. Majidi, A. Bouyanzer, J. Paolini, J. M. Desjobert, J. Costa, B. Hammouti. *Arab. J. Chem., 5* (2012) 467-474. https://doi.org/10.1016/j.arabjc.2010.09.017.
8. A. Khadraoui, A. Khelifa, H. Hamitouche, R. Mehdaoui. *Res. Chem. Intermed.,* 40 (2013) 961-972. https://doi.org/10.1007/s11164-012-1014-y.
9. R. Goel, W. A. Siddiqi, B. Ahmed, J. Hussan. *E-Journal Chem.,* 7 (2010) S319-S329. https://doi.org/10.1155/2010/308057.
10. M. B. Radovanović, M. B. Petrović, A. T. Simonović, S. M. Milić, M. M. Antonijević. *Environ. Sci. Pollut. Res.,* 20 (2013) 4370-4381. https://doi.org/10.1007/s11356-012-1088-5.
11. N. A. Odewunmi, S. A. Umoren, Z. M. Gasem. *J. Environ. Chem. Eng.,* 3 (2015) 286-296. https://doi.org/10.1016/j.jece.2014.10.014.
12. M. A. Dar. *Ind. Lubr. Tribol.,* 63 (2011) 227-233. https://doi.org/10.1108/00368791111140431.
13. I. F. Pérez-Ramírez, M. L. González-Dávalos, O. Mora, M. A. Gallegos-Corona, R. Reynoso-Camacho. *J. Funct. Foods*, 35 (2017) 24-31. https://doi.org/10.1016/j.jff.2017.05.028.
14. P. C. Okafor, I. E. Uwah, O. O. Ekerenam, U. J. Ekpe, *Pigment Resin Technol.,* 38 (2009) 236-241. https://doi.org/10.1108/03699420910973323.
15. S. A. Umoren, Z. M. Gasem, I. B. Obot. *Anti-Corrosion Methods Mater.,* 62 (2015) 19-28. https://doi.org/10.1108/ACMM-10-2013-1302.
16. M. Mehdipour, B. Ramezanzadeh, S. Y. Arman. *J. Ind. Eng. Chem.,* 21 (2015) 318-327. https://doi.org/10.1016/j.jiec.2014.02.041.
17. P. Muthukrishnan, B. Jeyaprabha, P. Prakash. *JMEP.*, 22 (2013) 3792-3800. https://doi.org/10.1007/s11665-013-0700-2.
18. Fdil, R.; Tourabi, M.; Derhali, S.; Mouzdahir, A.; Sraidi, K.; Jama, C.; Zarrouk, A.; Bentiss, F. *J. Mater. Environ. Sci.*, 9 (2018), 358-369. https://doi.org/10.26872/jmes.2018.9.1.39
19. Uwah, I.; Ikeuba, A.; Ugi, B.; Udowo, V. *Glob. J. Pure Appl. Sci., 19* (2013), 23-31. https://doi.org/10.4314/gjpas.v19i1.4
20. M. Y. Díaz-Cardenas, S. Lagunas-Rivera, V. M. Salinas-Bravo, J. G. Gonzalez-Rodríguez, M. G. Valladares-Cisneros, R. Lopez-Sesenes, *Green Chem. Lett. Rev.,* 10 (2017) 257-268. https://doi.org/10.1080/17518253.2017.1369167
21. G. M. J. Meyer, M. R. Meyer, D. K. Wissenbach, H. H. Maurer, *J. Mass Spectrom.,* 48 (2013) 24-41. https://doi.org/10.1002/jms.3112.
22. P. Kringstein, A. I. Cederbaum. *Free Radic. Biol. Med.,* 18 (1995) 559-563. https://doi.org/10.1016/0891-5849(95)91457-3.

23. P. O'Brien, C. Carrasco-Pozo, H. Speisky. *Chem Biol Interact*., 159 (2006) 1-17. https://doi.org/10.1016/j.cbi.2005.09.002.
24. M. A. Ameer, A. M. Fekry. *Prog. Org. Coatings,* 71 (2011) 343-349. https://doi.org/10.1016/j.porgcoat.2011.04.001.
25. E. A. Noor. *Mater. Chem. Phys.,* 114 (2009) 533-541. https://doi.org/10.1016/j.matchemphys.2008.09.065.
26. A. S. T. M. Standard practice for calculation of corrosion rates and related information from electrochemical measurements. In *Annual Book of ASTM standards*; (1994) 416-422.
27. E. Mc Cafferty. *Corros. Sci.,* 47 (2005) 3202-3215. https://doi.org/10.1016/j.corsci.2005.05.046.
28. M. Stern, A. L. Geary, *J. Electrochem. Soc.*, 104 (1957), 56. https://doi.org/10.1149/1.2428496.
29. E. McCafferty, *Corros. Sci.*, 47 (2005), 3202–3215. https://doi.org/10.1016/j.corsci.2005.05.046.
30. ASTM G102. Standard Practice for Calculation of Corrosion Rates and Related Information from Electrochemical Measurements. 1994.
31. J. Uruchurtu-Chavarin. *Corros.*, 47 (1991) 472-479. https://doi.org/10.5006/1.3585281.
32. D. K. Yadav, B. Maiti, M. A. Quraishi. *Corros. Sci.*, 52 (2010) 3586-3598. https://doi.org/10.1016/j.corsci.2010.06.0.
33. E. Poorqasemi, O. Abootalebi, M. Peikari, F. Haqdar. *Corros. Sci.,* 51 (2009) 1043-1054. https://doi.org/10.1016/j.corsci.2009.03.001.
34. W. J. Lorenz and F. Mansfeld. *Corr. Sci.* 21(1981) 647-672. https://doi.org/10.1016/0010-938X(81)90015-9.
35. X. Cheng. *J. Electrochem. Soc.,* 145 (1998) 352. https://doi.org/10.1149/1.1838259.
36. I. Ahamad, M. A. Quraishi. *Corros. Sci.* 2010, 52 (2), 651-656. https://doi.org/10.1016/j.corsci.2009.10.012
37. Y. Lu, H. Xu, J. Wang, X. Kong. *Electrochim. Acta,* 54 (2009) 3972-3978. https://doi.org/10.1016/j.electacta.2009.02.019
38. Y. M. Tang, Y. Chen, W. Z. Yang, Y. Liu, X. S. Yin, J. T. Wang. *J. Appl. Electrochem.*, 38 (2008) 1553-1559. https://doi.org/10.1007/s10800-008-9603-6.
39. W. H. Smyrl. Electrochemistry and Corrosion on Homogeneous and Heterogeneous Metal Surfaces. In: J. O. Bockris, B. E. Conway, E. Yeager, R. E. White (eds) Electrochemical Materials Science. Comprehensive Treatise of Electrochemistry, vol 4, Springer, Boston, MA ISBN: 978-1-4757-4825-3(1981) 97-149.
40. G. Quartarone, T. Bellomi, A. Zingales. *Corros. Sci.,* 45 (2003), 715-733. https://doi.org/10.1016/S0010-938X(02)00134-8.
41. G. L. F. Mendonça, S. N. Costa, V. N. Freire, P. N. S. Casciano, A. N. Correia, P. de Lima-Neto. *Corros. Sci.*, 115 (2017), 41-55. https://doi.org/10.1016/j.corsci.2016.11.012
42. G. Quartarone, T. Bellomi, A. Zingales. *Corros. Sci.*, 45 (2003) 715-733. https://doi.org/10.1016/S0010-938X(02)00134-8.
43. G. Moretti, F. Guidi. *Corros. Sci.*, 44 (2002) 1995-2011. https://doi.org/10.1016/S0010-938X(02)00020-3.
44. I. D. Raistrick, D. R. Franceschetti, J. R. Macdonald, Impedance spectroscopy, in: E. Barsoukov, J. R. Macdonald (Eds.), Theory, Experimental and Applications, 2nd ed., John Wiley & Sons, New Jersey (2005).
45. G. L. F. Mendonça, S. N. Costa, V. N. Freire, P. N. S. Casciano, A. N. Correia, P. de Lima-Neto. *Corros. Sci.*, 115 (2017) 41-55. https://doi.org/10.1016/j.corsci.2016.11.012.
46. J. B. Jorcin, M. E. Orazem, N. Pébère, B. Tribollet. *Electrochim. Acta,* 51 (2006) 1473-1479. https://doi.org/10.1016/j.electacta.2005.02.128.
47. E. Barsoukov, J. R. Macdonald. Impedance Spectroscopy Theory, Experiment, and Applications, 2nd ed. Hoboken, NJ: John Wiley & Sons, Inc. ISBN: 0-471-64749-7 (2005).
48. S. Shahabi, P. Norouzi, M. R. Ganjali. *RSC Adv.*, 5 (2015) 20838-20847. https://doi.org/10.1039/c4ra15808c
49. C. Kamal, M. G. Sethuraman. *Res. Chem. Intermed.*, 39 (2013) 3813-3828. https://doi.org/10.1007/s11164-012-0883-4.
50. J. M. Smith. Chemical Engineering Kinetics, 2nd; McGraw-hill, New York, ISBN: 13: 978-0070665743(1970).
51. M. Bouklah, B. Hammouti, A. Aouniti, M. Benkaddour, A. Bouyanzer. *Appl. Surf. Sci.*, 252 (2006) 6236-6242. https://doi.org/10.1016/j.apsusc.2005.08.026.
52. A. Zingales, G. Quartarone, T. Bellomi, G. Moretti, G. Capobianco. *Corros.,* 54 (2010) 606-618. https://doi.org/10.5006/1.3287636.

53. M. A. Sudheer, M. A. Quraishi, Corros. Sci., 70 (2013) 161-169. https://doi.org/10.1016/j.corsci.2013.01.025.

54. M. Hosseini, S. F. L. Mertens, M. Ghorbani, M. R. Arshadi. *Mater. Chem. Phys.,* 78 (2003) 800-808. https://doi.org/10.1016/S0254-0584(02)00390-5.

55. H. B. Ouici, O. Benali, A. Guendouzi. *Res. Chem. Intermed.*, 42 (2016), 7085-7109. https://doi.org/10.1007/s11164-016-2520-0.

56. A. El Bribri, M. Tabyaoui, B. Tabyaoui, H. El Attari, F. Bentiss. *Mater. Chem. Phys.,* 141 (2013) 240-247. https://doi.org/10.1016/j.matchemphys.2013.05.006

57. G. Bereket, E. Hür, C. Öretir. *J. Mol. Struct. THEOCHEM*, 578 (2002) 79-88. https://doi.org/10.1016/S0166-1280(01)00684-4.

58. A. Zarrouk, B. Hammouti, A. Dafali, F. Bentiss. *Ind. Eng. Chem. Res.*, 52 (2013), 2560-2568. https://doi.org/10.1021/ie301465k.

59. I. B. Obot, D. D. Macdonald, Z. M. Gasem. *Corros. Sci.,* 99 (2015) 1-30. https://doi.org/10.1016/j.corsci.2015.01.037.

60. N. O. Obi-Egbedi, I. B. Obot. Corros. Sci., 53 (2011) 263-275. https://doi.org/10.1016/j.corsci.2010.09.020.

61. A. Kokalj. Electrochim. Acta, 56 (2010) 745-755. https://doi.org/10.1016/j.electacta.2010.09.065.

62. A. Srivastava, P. Tandon, A. P. Ayala, S. Jain. *Vib. Spectrosc.*, 56 (2011) 82-88. https://doi.org/10.1016/j.vibspec.2010.08.001.

63. B. Ramaganthan, M. Gopiraman, L. O. Olasunkanmi, M. M. Kabanda, S. Yesudass, I. Bahadur, A. S. Adekunle, I. B. Obot, E. E. Ebenso. *RSC Adv.,* 5 (2015) 76675-76688. https://doi.org/10.1039/c5ra12097g

64. J. Bhawsar, P. Jain, M. G. Valladares-Cisneros, C. Cuevas-Arteaga. Bhawsar, M. R. *Int. J. Electrochem. Sci.*, 13 (2018) 3200-3209. https://doi.org/10.20964/2018.04.57.

65. A. Kokalj. *Chem. Phys.*, 393 (2012) 1-12. https://doi.org/10.1016/j.chemphys.2011.10.021.

66. H. Lgaz, K. Subrahmanya Bhat, R. Salghi, Shubhalaxmi; S. Jodeh, M. Algarra, B. Hammouti, I. Hassan Ali, A. Essamri. *J. Mol. Liq.*, 238 (2017) 71-83. https://doi.org/10.1016/j.molliq.2017.04.124.

(2019) ; http://www.jmaterenvironsci.com